

# Alignment of MG-63 Osteoblasts on Fibronectin-Coated Phosphorous Doping Lattices in Silicon

Andreas Körtge, Susanne Stählke, Regina Lange, Mario Birkholz, Mirko Fraschke, Katrin Schulz, Barbara Nebe, and Patrick Elter

**Abstract**—A major challenge in biomaterials research is the regulation of protein adsorption which is a key factor for controlling the subsequent cell adhesion at implant surfaces. The aim of the present study was to control the adsorption of fibronectin (FN) and the attachment of MG-63 osteoblasts with an electronic nanostructure. Shallow doping line lattices with a period of 260 nm were produced for this purpose by implantation of phosphorous in silicon wafers. Protein coverage was determined after incubating the substrate with FN by means of an immunostaining procedure and the measurement of the fluorescence intensity with a TECAN analyzer. We observed an increased amount of adsorbed FN on the nanostructure compared to control substrates. MG-63 osteoblasts were cultivated for 24h on FN-incubated substrates and their morphology was assessed by SEM. Preferred orientation and elongation of the cells in direction of the doping lattice lines was observed on FN-coated nanostructures.

**Keywords**—Cell adhesion, electronic nanostructures, doping lattice, fibronectin, MG-63 osteoblasts, protein adsorption.

## I. INTRODUCTION

PROTEIN adsorption as the first step of biomaterial-biosystem interaction is a key factor for controlling the subsequent cell adhesion and the function of adherent cells [1]. The adsorption process is influenced by characteristics of the protein, the substrate, and the surrounding aqueous solution. In respect of the material properties surface chemistry [2], [3], topography [2], [4] and wettability [5], [6] are known to affect the adsorption behavior. However, it is not fully understood to which extent each of these factors contributes to the adsorption process of proteins. In order to study the influence of the different factors separately simplified model systems with well-defined physicochemical material properties are necessary. We used a phosphorous doping line lattice to generate a defined modulation of the near-surface electric field strength which was expected to affect the adsorption behavior of proteins. In addition to this the wettability of the substrates was determined by means of optical contact measurements. Because of its high sensitivity towards the local micro environment [4] and its major importance in cell adhesion FN was chosen for our study. Initially the influence of the doping lattice on the adsorption

A. Körtge, R. Lange, and P. Elter are with the Institute of Electronic Appliances and Circuits, University of Rostock, Rostock, Germany (Corresponding author A. Körtge; phone: +49-381-492-7240; fax: +49-381-498-118-7233; e-mail: andreas.koertge@uni-rostock.de).

S. Stählke and B. Nebe are with the Department of Cell Biology, University of Rostock, Rostock, Germany.

M. Birkholz, M. Fraschke and K. Schulz are with the IHP GmbH, Frankfurt (Oder), Germany.

behavior of FN was investigated by incubating the substrates, tagging immobilized protein molecules with an indirect immunostaining procedure, and quantifying the intensity of the fluorescent dye. The next step was then to determine the influence of this FN coating on the morphology of adherent MG-63 osteoblasts by SEM top view images.

## II. METHODS

### A. Substrate Preparation and Characterization

Doping lattices were inscribed into silicon wafers as outlined in detail in the work of Birkholz et al. [7]. 200 mm p-type CZ-Si with  $\langle 100 \rangle$  orientation and 5-20 m $\Omega$ cm served as starting material. In contrast to the work of Birkholz et al. [7] the electronic nanostructures were produced in this work by doping 130 nm wide stripes with phosphorous instead of arsine. Doping was achieved by implanting 20 keV P ions with a dose of  $3 \times 10^{15}$  cm $^{-2}$ . The doping lattice sample was prepared by firstly depositing a SiO $_2$ /SiN double layer, having the main purpose to act as an anti-reflection coating in order to improve the spatial resolution of the subsequent lithographic process. A 5 nm oxide layer was grown by thermal oxidation, which was followed by a chemical-vapour deposition of 25 nm silicon nitride. Line lattices were prepared by photolithography with a dedicated reticule. A combination of a Nikon NSR S207D Scanner for exposure of intentionally doped areas and a TEL track for deposition and development of photo resist was used for this purpose. UV 2000 resist with a thickness of 335 nm was applied in this study, which was exposed by a dose of 50.2 mJ and developed with NMD-W. Phosphorous ions were implanted in the subsequent process step through the SiO $_2$ /SiN double layer only in resist-free areas. Their energy was adequately chosen such that a doping density of  $10^{20}$  cm $^{-3}$  at depths of less than 50 nm below the wafer surface was finally achieved. These were followed by an annealing step for recrystallization of amorphous regions and etch steps for removing photo resist, SiN and SiO $_2$ . All process steps were derived from full semiconductor technology flows established at IHP for preparing 0.25  $\mu$ m and 0.13  $\mu$ m CMOS/BiCMOS microelectronic circuits [8], [9]. The starting material (Si control) and a homogeneously P-doped wafer (P control) served as reference substrates.

The influence of the selective phosphorous doping on the topography and surface potential distribution of the electronic nanostructure under ambient conditions was determined by means of atomic force microscopy (AFM)-based Kelvin probe force microscopy (KPFM). The AFM measurements were performed with a JPK Nanowizard II (JPK Instruments,

Berlin, Germany) and doped silicon cantilevers with a nominal tip radius of 10 nm (42 N/m force constant; NCH, NanoWorld, Neuchâtel, Switzerland). In the trace direction of the KPFM mode the topography was measured in intermittent contact (IC) mode with a scan rate of 1 Hz. In the retrace direction solely an AC voltage ( $V_{p-p} = 0.2$  V) with the same frequency as the mechanical excitation was applied and the cantilever tip scanned the surface in a constant distance of 20 nm.

Additionally, the static contact angle of distilled water (sessile drop, 0.5  $\mu$ L) was determined with an optical contact angle measurement system (OCA 15EC, DataPhysics Instruments GmbH, Germany). Immediately before conducting the contact angle and the biological experiments the samples were cleaned. For that purpose the specimens were sonicated for 10 min in acetone, isopropyl alcohol, ethanol (p.a.) and finally for 30 min in distilled water.

#### B. Staining Procedure and Fluorescence Quantification

The substrates were incubated with bovine plasma FN (Sigma-Aldrich, Germany) at a bulk concentration of 10  $\mu$ g/mL in Dulbecco's Phosphate Buffered Saline (DPBS 1x, w/o Ca & Mg ions; PAA Laboratories, Cölbe, Germany) for 2h. Subsequently the substrates were incubated with 2% bovine serum albumin (BSA, Sigma-Aldrich, Germany) for 30 min in order to avoid nonspecific binding of antibodies to the surface. After the blocking with BSA a primary anti-FN antibody (H-300; Santa Cruz Biotechnology, Heidelberg, Germany), which binds to the C terminus of bovine FN, in 1% BSA was added. An appropriate secondary antibody coupled to a fluorescent dye (goat anti-rabbit IgG-CFL 488; Santa Cruz Biotechnology, Heidelberg, Germany) in 1% BSA was used to tag the primary antibody. In order to remove any non-adsorbed FN and non-specifically bound antibodies the substrates were gently rinsed with DPBS three times after each procedure step. Furthermore, controls of all three substrate modifications were incubated with 2% BSA in DPBS in order to assure the specific binding of the primary and secondary antibodies to the FN epitope and the primary antibody, respectively. The quantification of the FN covering was conducted with a Tecan multiwell plate reader (Tecan Group Ltd., Switzerland): the fluorescent dye was excited at 488 nm with a UV xenon flash lamp (double monochromatized light, bandwidth < 9 nm) and the emission signal was measured at 519 nm for 20  $\mu$ s with a photomultiplier tube after again being double monochromatized (bandwidth < 20 nm).

#### C. Cell Culture and Morphology Evaluation

Human osteoblastic cells (MG-63, ATCC, CRL-1427) were cultured in Dulbecco's modified Eagle medium (DMEM, Invitrogen GmbH, Karlsruhe, Germany) with a density of  $3 \times 10^4$  cells/array in a humidified atmosphere with 5%  $\text{CO}_2$  on FN-incubated (10  $\mu$ g/mL in DPBS) and non-incubated substrates. After 24 h cultivation time the cells were washed with DPBS, fixed with 2.5% glutaraldehyde (4°C; Merck, Darmstadt, Germany), rinsed with NaP-buffer, and dehydrated through a graded series of acetone (30% 5 min, 50% 5 min,

75% 10 min, 90% 15 min, 100% twice for 10 min). After being dried in a critical point dryer (K850, EMITECH, Taunusstein, Germany) the samples were sputter coated with 12 nm gold (SCD004, BAL-TEC, Macclesfield, UK) and the cell morphology was examined with a field emission scanning electron microscope (FE-SEM SUPRA 25, Carl Zeiss, Germany).

### III. RESULTS

#### A. Substrate Characterization

##### 1) KPFM Measurements

The topography scan of the doping lattice and the associated KPFM signal map under ambient conditions are depicted in Fig. 1 (a) and Fig. 1 (b), respectively. We observed a slight topographical variation of approximately 10 nm and a surface potential variation of 250 mV which leads to an estimated variation of the electric field strength perpendicular to the lattice lines in the range of  $10^6$  to  $10^7$   $\text{Vm}^{-1}$  due to the small dimensions of the doping lattice. Moreover, by comparing the topography and the KPFM map it becomes apparent that the grooves of the nanostructure exhibit a more positive surface potential than the summits.

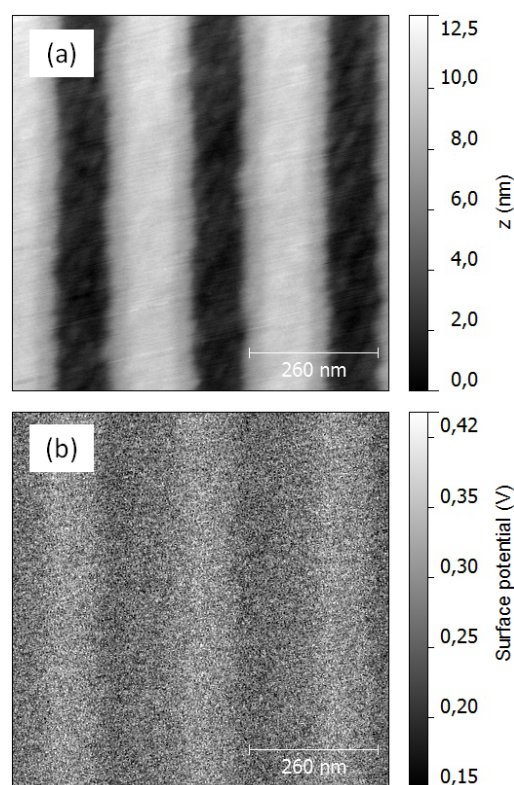


Fig. 1 (a) Topography and (b) the associated surface potential map of the phosphorous doping lattice measured with AFM-based KPFM

##### 2) Contact Angle Measurements

The water contact angle of the three substrate modifications is depicted in Fig. 2. The diagram indicates that the surface hydrophobicity is significantly increased in a nearly linear manner with an increase of the P-doped area: in comparison to

the starting wafer (Si control, 0% P-doped area) the contact angle is doubled by the doping lattice (50% P-doped area) and tripled by the homogeneously doped wafer (P control, 100% P-doped area).

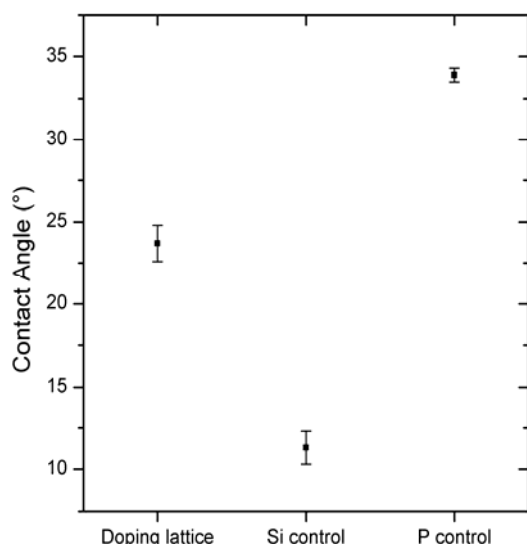


Fig. 2 Contact angle of distilled water on the phosphorous doping lattice compared to the control substrates (mean  $\pm$  standard deviation, n=3)

#### B. Immunofluorescence Measurements

In Fig. 3 the fluorescence intensity of the adsorbed and stained FN is depicted. It shows a significantly increased ( $p < 0.05$ ) amount of adsorbed FN on the doping lattice compared to the control substrates whereas no significant difference was observed between the controls.

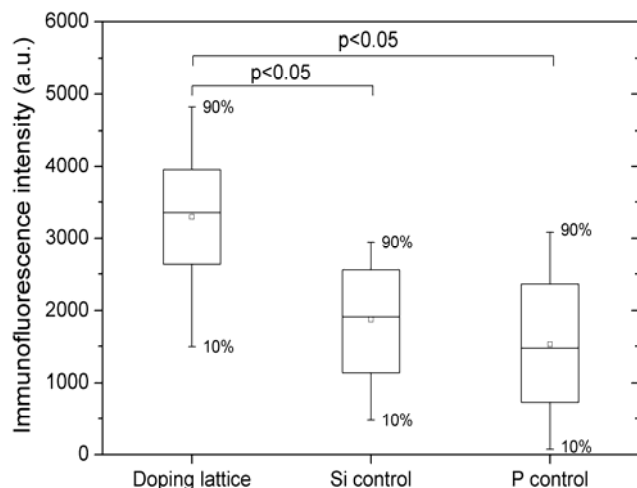


Fig. 3 Quantification of the adsorbed FN on the phosphorous doping lattice compared to two control substrates (starting wafer - Si control; homogeneously P-doped wafer - P control) (Mann-Whitney U test, n=80)

#### C. Cell Morphology

Fig. 4 shows the morphology of MG-63 osteoblasts cultivated for 24h on a phosphorous doping lattice which was previously incubated with a bulk FN concentration of

10  $\mu\text{g/mL}$  in DPBS. The SEM top view indicates that the cells elongate and orientate in direction of the doping lattice lines in combination with a FN coating whereas no alignment was observed when the FN incubation was omitted.

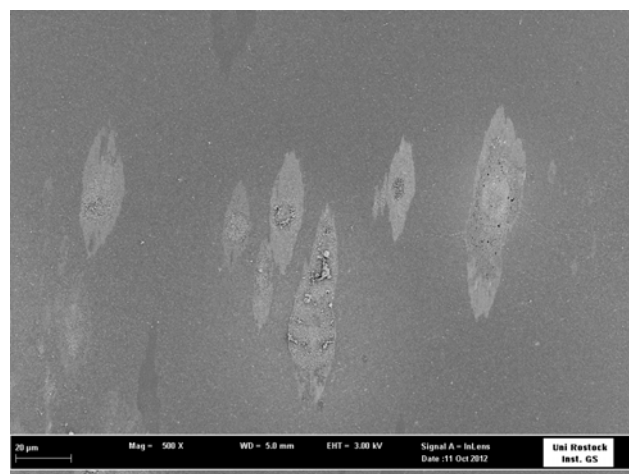


Fig. 4 SEM top view of MG-63 osteoblasts attached to the previously FN-incubated (10  $\mu\text{g/mL}$ ) phosphorous doping lattice after 24h cultivation time. The white arrow indicates the direction of the lattice lines

#### IV. DISCUSSION

In the present work we used a phosphorous doping lattice to control the FN adsorption behavior which was assessed by immunofluorescence measurements. Due to a surface potential variation of approximately 250 mV and the small structure size of the doping lattice a variation of the near-surface electric field strength in the range of  $10^6$  to  $10^7 \text{ Vm}^{-1}$  is estimated. The occurrence of the topographic variation is assigned to the combined effects of stress relief and preferred etching of ion-damaged and recrystallized surface areas [7]. Compared to the starting wafer and the homogeneously P-doped wafer the amount of adsorbed FN is significantly increased on the doping lattice for a bulk FN concentration of 10  $\mu\text{g/mL}$ . Our results indicate that this influence of the electronic nanostructure is caused by a superposition of topographic effects and the modulation of the near-surface electric field strengths since the same amount of adsorbed fibronectin was found on the starting wafer (Si control) as well as on the homogeneously P-doped wafer (P control). Accordingly, the dopant itself seems to have no effect on the protein adsorption, although the more hydrophobic nature of the P control was expected to induce an increased amount of adsorbed FN [10]. The results of the cell experiments indicate that the electronic nanostructure in combination with a FN coating is a promising approach to control the cell attachment: a majority of MG-63 osteoblasts on the FN-incubated doping lattice orientated and elongated in direction of the lattice lines whereas no alignment was observed without previous protein incubation. The influence of the electronic nanostructure on the cells is somehow mediated by the state of the adsorbed FN molecules.

#### ACKNOWLEDGMENT

We thank the German Research Foundation for financially supporting this work within the framework of the research training group “Welisa” (DFG 1505/1).

#### REFERENCES

- [1] C.J. Bettinger, R. Langer, J.T. Borenstein, Engineering Substrate Topography at the Micro- and Nanoscale to Control Cell Function, *Angew. Chem. Int. Ed.* 48 (2009) 5406–5415.
- [2] C. Galli, M.C. Coen, R. Hauert, V.L. Katanaev, M.P. Wymann, P. Gröning, L. Schlapbach, Protein adsorption on topographically nanostructured titanium, *Surface Science* 474 (2001) L180-L184.
- [3] P. Roach, D. Farrar, C.C. Perry, Surface Tailoring for Controlled Protein Adsorption: Effect of Topography at the Nanometer Scale and Chemistry, *J. Am. Chem. Soc.* 128 (2006) 3939–3945.
- [4] P. Elter, R. Lange, U. Beck, Atomic force microscopy studies of the influence of convex and concave nanostructures on the adsorption of fibronectin, *Colloids and surfaces* 89 (2012) 139–146.
- [5] G.B. Sigal, M. Mrksich, G.M. Whitesides, Effect of Surface Wettability on the Adsorption of Proteins and Detergents, *J. Am. Chem. Soc.* 120 (1998) 3464–3473.
- [6] Y. Arima, H. Iwata, Effect of wettability and surface functional groups on protein adsorption and cell adhesion using well-defined mixed self-assembled monolayers, *Biomaterials* 28 (2007) 3074–3082.
- [7] M. Birkholz, P. Zaumseil, J. Bauer, D. Bolze, G. Weidner, Small-angle reciprocal space mapping of surface relief gratings, *Materials science & engineering* 27 (2007) 1154–1157.
- [8] D. Knoll, K. Ehwald, B. Heinemann, A. Fox, K. Blum, H. Rucker, F. Furnhammer, B. Senapati, R. Barth, U. Haak, W. Hoppner, J. Drews, R. Kurps, S. Marschmeyer, H. Richter, T. Grabolla, B. Kuck, O. Fursenko, P. Schley, R. Scholz, B. Tillack, Y. Yamamoto, K. Kopke, H. Wulf, D. Wolansky, W. Winkler, A flexible, low-cost, high performance SiGe:C BiCMOS process with a one-mask HBT module, pp. 783–786.
- [9] D. Knoll, B. Heinemann, R. Barth, K. Blum, J. Borngraber, J. Drews, K.-E. Ehwald, G. Fischer, A. Fox, T. Grabolla, U. Haak, W. Hoppner, F. Korndorfer, B. Kuck, S. Marschmeyer, H. Richter, H. Rucker, P. Schley, D. Schmidt, R. Scholz, B. Senapati, B. Tillack, W. Winkler, D. Wolansky, C. Wolf, H.-E. Wulf, Y. Yamamoto, P. Zaumseil, A modular, low-cost SiGe:C BiCMOS process featuring high- $f$ /sub T/ and high BV/sub CEO/ transistors, pp. 241–244.
- [10] F. Grinnell, M.K. Feld, Fibronectin adsorption on hydrophilic and hydrophobic surfaces detected by antibody binding and analyzed during cell adhesion in serum-containing medium, *J. Biol. Chem.* 257 (1982) 4888–4893.